

September 27, 2017

Are Seyfert Narrow Line Regions Powered by Radio Jets?

Geoffrey V. Bicknell ¹, Michael A. Dopita ², Zlatan I. Tsvetanov ³, Ralph S. Sutherland ¹

Submitted to the Astrophysical Journal, Sept. 4, 1997

¹ANU Astrophysical Theory Centre, Australian National University, Canberra, ACT 0200, Australia. The ANUATC is operated jointly by the Mt. Stromlo and Siding Spring Observatories and the School of Mathematical Sciences of the Australian National University.

²Mount Stromlo & Siding Spring Observatories, Weston PO, ACT 2611, Australia

³Dept. of Physics & Astronomy, Johns Hopkins University, Baltimore, MD 21218, USA

ABSTRACT

We argue that the narrow line regions of Seyfert galaxies are powered by the transport of energy and momentum by the radio-emitting jets. This implies that the ratio of the radio power to jet energy flux is much smaller than is usually assumed for radio galaxies. This can be partially attributed to the smaller ages ($\sim 10^6$ yrs) of Seyferts compared to radio galaxies but one also requires that either the magnetic energy density is more than an order of magnitude below the equipartition value, or more likely, that the internal energy densities of Seyfert jets are dominated by thermal plasma, as distinct from the situation in radio galaxy jets where the jet plasma is generally taken to be nonthermally dominated. If the internal energy densities of Seyfert jets are initially dominated by relativistic plasma, then an analysis of the data on jets in five Seyfert galaxies shows that all but one of these would have mildly relativistic jet velocities near 100 pc in order to power the respective narrow-line regions. However, observations of jet-cloud interactions in the NLR provide additional information on jet velocities and composition via the momentum budget. Our analysis of a jet-cloud interaction in NGC 1068, 24 pc from the core, implies a shocked jet pressure much larger than the minimum pressure of the radio knot, a velocity (probably accurate to within a factor of a few) $\sim 0.06 c$ (18,000 km s $^{-1}$) and a temperature of thermal gas in the jet $\sim 10^9$ K implying mildly relativistic electrons but thermal protons. The estimated jet velocity is proportional to the jet energy flux and provides an independent argument that the energy flux in the northern NGC 1068 jet is much greater than previously supposed and is capable of providing significant energy input to the narrow line region. The jet mass flux at this point $\sim 0.5 M_{\odot} \text{ yr}^{-1}$, is an order of magnitude higher than the mass accretion rate $\sim 0.05 M_{\odot} \text{ yr}^{-1}$ estimated from the bolometric luminosity of the nucleus, strongly indicating entrainment into the jet and accompanying deceleration. Consequently, the jet velocity near the black hole is likely to be mildly relativistic. We estimate an initial jet mass flux $\sim 0.02 M_{\odot} \text{ yr}^{-1}$ which is comparable to the mass accretion rate. This mass flux is consistent with the densities inferred for accretion disc coronae from high energy observations, together with an initially mildly relativistic velocity and an initial jet radius of order 10 gravitational radii.

1. Introduction

The dominant paradigm for the excitation of emission lines in the narrow line regions (NLRs) of Seyfert galaxies invokes photoionization by a central power-law continuum. The apparent lack of ionizing photons in Seyfert 2s has been attributed to obscuration by a thick torus surrounding the central region of the Active Galactic Nucleus (AGN). Nevertheless, Binette, Fosbury, & Parker (1993) have argued that there is a deficit of ionizing photons in *all* AGN leading to some scepticism of central power-law photoionization. On the other hand, it has been recognized for some time (Binette, Dopita, & Tuohy 1985) that excitation by autoionizing shocks in various classes of AGN can give a reasonable fit to the observed spectra and improve the agreement between theory and observation for the temperature-sensitive [OIII] λ 4363 line. Notable individual successes of this approach include a self-consistent model for the excitation of the emission line filaments in Centaurus A (Sutherland, Bicknell, & Dopita 1993) and the excitation of the disk in the central 100 pc of M87 (Dopita et al. 1997). In the latter case, detection by HST of high excitation lines in the ultraviolet together with the excellent agreement between the observed and predicted spectra make a strong case for shock excitation. Bicknell, Dopita, & O’Dea (1997) have also shown that the narrow-line emission from Gigahertz Peak Spectrum (GPS) and Compact Steep Spectrum (CSS) radio sources can plausibly be related to the excitation of a dense ISM by the bow shock surrounding the radio source. That model has the additional feature of providing a natural explanation for the peak in the radio spectrum of these sources. Koekemoer & Bicknell (1997) have also made a strong case for the shock excitation of the extended emission-line region in the radio galaxy PKS2356-61. For Seyfert galaxies, Viegas & Contini (1997) have also suggested that emission lines from shocked gas in cloud-cloud collisions constitute a fraction of the total emission line output from the narrow line region (NLR). In view of the increasing interest in autoionizing shocks, a grid of models of shock excited spectra has been calculated (Dopita & Sutherland 1996a; Dopita & Sutherland 1996b). These provide a good description of the observed spectra.

The correlation between radio power and [OIII] λ 5007 luminosity in Seyfert galaxies discovered by Whittle (1985) over twelve years ago, suggests an intimate connection between the radio-emitting and emission-line components. Indeed, where observations are made at high enough resolution, detailed correspondence between radio and optical features is often found, along with evidence of dynamical structure and sources of local ionization indicative of shocks (Whittle et al. (1988), Goodrich (1992, Capetti et al. (1996)). In the specific case of NGC 1068 Capetti, Axon, & Machetto (1997) have shown, using HST/WFPC2 [OIII] and $H\alpha$ + [NII] images overlaid on a VLA radio image of the radio source, that there is a close correspondence between the radio and optical structure, strongly supporting the view that the NLR of NGC 1068 is the result of interaction with the radio plasma. Another key observation is that the radio axes of Seyferts correspond remarkably to the axes of their ionization cones, again suggesting that the radio and optical emission are causally related (Wilson & Tsvetanov 1994). The view advocated here is that the Whittle radio–optical luminosity correlation together with the unequivocal morphological correlations between radio and line-emitting gas is strong circumstantial evidence

that the mechanical energy and momentum transported by the radio plasma is responsible for the excitation of at least some, and probably most, of the narrow-line region (NLR). An alternative interpretation of a similar correlation for radio galaxies was given by Rawlings & Saunders (1991) who suggested that the accretion disk luminosity (as indicated by the NLR [OIII] luminosity) and the mechanical luminosity of the jet are correlated. This suggestion was taken up by Falcke & Biermann (1995) and Falcke, Malkan, & Biermann (1995) who proposed that a substantial fraction of the energy dissipated by all AGN accretion disks finds its way into jet mechanical luminosity. However, this view does not really represent an alternative, since the inferred jet energy flux is comparable to the ionizing luminosity of the accretion disk and capable of having an important influence on the energy budget of the NLR gas.

If the narrow line emission from Seyfert galaxies is to be powered by the expansion of the radio lobe, then, appealing to the GPS/CSS model of Bicknell, Dopita, & O’Dea (1997) as a basis for order of magnitude estimates, the [OIII] λ 5007 luminosity is given by

$$L([OIII]) \approx 1.0 \times 10^{-2} \left(\frac{6}{8 - \delta} \right) F_E \text{ ergs s}^{-1} \quad (1-1)$$

where δ is the power-law index of the ambient density distribution and F_E is the combined energy flux in both jets. Hence, a median Seyfert [OIII] luminosity $\sim 10^{42}$ ergs s^{-1} requires an energy flux in each jet $\sim 5 \times 10^{43}$ ergs s^{-1} . Thus, a major argument *against* the nonthermal plasma powering the emission-line region (e.g.. Wilson (1997)) is based upon the low radio luminosity of Seyferts (typically $\sim 10^{23}$ W Hz^{-1} at 5 GHz). Using standard conversion factors relating radio luminosity and mechanical jet power used for radio galaxies, one finds that the jet power falls short of what is required by at least two orders of magnitude. In earlier papers (e.g.. Bicknell (1995), Bicknell, Dopita, & O’Dea (1997)), we have represented this conversion factor by κ_ν , the ratio of monochromatic power at frequency ν to jet energy flux. The advantage of using this parameter is that it is easily estimated using straightforward physics. The correlation between [OIII] λ 5007 luminosity and 1.4 GHz radio power is represented in Figure 1 where the correlation is plotted for a number of radio loud objects (used by Bicknell, Dopita, & O’Dea (1997)) together with the Seyferts in Whittle’s sample. The lines represent the theoretical relationship between [OIII] luminosity and radio power predicted by the GPS/CSS model of Bicknell, Dopita, & O’Dea (1997). The values of $\log \kappa_{1.4}$ (where $\kappa_{1.4}$ represents κ_ν at a frequency of 1.4 GHz) range from -14 (extreme left) to -10 (extreme right). Seyferts are separated quite clearly from the radio loud objects by, on average, three or even four orders of magnitude in $\kappa_{1.4}$

In this paper, we examine the question of whether Seyferts are in fact characterized by such low values of $\kappa_{1.4}$ and additional aspects of the energy and momentum budgets which have a strong bearing on the question of whether jets can power the NLR of Seyfert galaxies. Some of the following analysis is specific to NGC 1068 and the case of this galaxy, we examine the dynamical link between the jet parameters and the expected parameters of the corona above the accretion disk in the vicinity of the black hole.

2. The Relation between Jet Power and Radio Luminosity.

Traditionally, an effective value of κ_ν has been based on an assumed “efficiency of conversion” of jet power into total radio luminosity. However, this “efficiency factor” has a physical basis (Bicknell (1984), Eilek & Shore (1989), Bicknell (1995), Begelman (1996), Bicknell, Dopita, & O’Dea (1997)). For convenience, we summarize here the physics of this relationship as given by Bicknell, Dopita, & O’Dea (1997). Consider a jet-fed radio lobe: The total energy, E_L accumulating in the lobe can be represented approximately as $f_{\text{ad}} F_E t$ where F_E is the jet energy flux, t is the age of the lobe and $f_{\text{ad}} \sim 0.5$ is a factor which accounts for the energy lost adiabatically by expansion⁴. The synchrotron emission from the lobe is given by $P_\nu \approx C_{\text{syn}}(a) K B^{(a+1)/2} \nu^{-(a-1)/2} V$ where C_{syn} is expressed in terms of the Pacholczyk (1970) synchrotron parameters, c_i by $C_{\text{syn}}(a) = 4\pi c_5(a) c_9(a) (2c_1)^{(a-1)/2}$, the electron energy density per unit energy, $N(E)$, is given by $N(E) = K E^{-a}$, B is the (randomly oriented) magnetic field, ν is the observing frequency, and V is the volume. The parameter K can be expressed in terms of the electron/positron energy density, ϵ_e via $K = (a - 2)\epsilon_e(\gamma_0 m_e c^2)^{(a-2)} [1 - (\gamma_1/\gamma_0)^{-(a-2)}]^{-1}$ where γ_0 and γ_1 are respectively the lower and upper Lorentz factor cutoffs in the electron distribution. Writing the total electron/positron energy in the lobe as $f_e E_L$ where f_e is the electron/positron fraction of the total energy, we obtain for the ratio of monochromatic radio power to jet energy flux:

$$\kappa_\nu \approx (a - 2) C_{\text{syn}}(a) (\gamma_0 m_e c^2)^{(a-2)} \left[1 - (\gamma_1/\gamma_0)^{-(a-2)} \right]^{-1} f_e f_{\text{ad}} B^{(a+1)/2} t \quad (2-1)$$

The most important factors in this equation are (1) the electron/positron fraction, f_e , (2) the magnetic field, B and (3) the age, t . This relationship is plotted in Figure 2 for a range of values of the evolutionary parameter $\tau = f_e f_{\text{ad}} t$, assuming $\gamma_0 = 1$, $\gamma_1 = \infty$, a spectral index of 0.7 and an observing frequency of 1.4 GHz. The band of $\kappa_{1.4}$ ($-15 \lesssim \log \kappa_{1.4} \lesssim -13$) which we suggest is relevant to Seyferts is indicated. For example a value of $\kappa_{1.4} \sim 10^{-13}$ and radio power $\sim 10^{23} \text{ W Hz}^{-1}$ indicates a combined jet energy flux $\sim 10^{43} \text{ ergs s}^{-1}$. From the plot it is evident that the values of B and τ which are most conducive to $\kappa_{1.4}$ lying in this range are in the vicinity of $B \sim 10^{-5} - 10^{-4} \text{ G}$ and corresponding values of $\tau \sim 10^6 - 10^4 \text{ yrs}$. Typical equipartition magnetic fields and dynamical ages for Seyfert galaxies are approximately 10^{-4} G and 10^6 yrs (Wilson 1997), respectively, so that values of B and τ in the required range are feasible. However, if $\tau \sim 10^6 \text{ yrs}$ the magnetic field is required to be approximately an order of magnitude below equipartition. If the magnetic field is at equipartition we require $\tau \sim 10^4 \text{ yrs}$. The latter would be the case if τ is less than the dynamical age as a result of dominance of the thermal pressure (compared to the nonthermal) making $f_e \lesssim 0.1$. Thus this analysis raises the prospect that Seyfert jets, on the kpc scale, are dominated by thermal gas as distinct from radio galaxy and quasar jets which are normally taken to be dominated by nonthermal plasma.

A related way of looking at this question is to ask whether the typical equipartition pressures inferred for the lobes of Seyfert galaxies are capable of driving the $\sim 500 \text{ km s}^{-1}$ shocks necessary

⁴ $f_{\text{ad}} = 1$ if there is no energy lost by expansion.

to explain the optical and UV emission line spectrum. The pressure required to drive a shock of velocity V_{sh} into gas with pre-shock density ρ_{ps} is $\rho_{\text{ps}}V_{\text{sh}}^2 \approx 6 \times 10^{-8} (n_{\text{ps}}/10\text{cm}^{-3}) (V_{\text{sh}}/500\text{kms}^{-1})^2$ where n_{ps} is the pre-shock Hydrogen density. In order to produce the typical [SII] densities $\sim 10^{3-4} \text{cm}^{-3}$ inferred for NLR clouds we require $n_{\text{ps}} \gtrsim 10 \text{cm}^{-3}$ requiring driving pressures $\gtrsim 10^{-7} \text{dyn cm}^{-2}$ well above the typical values of $\sim 10^{-9} \text{dyn cm}^{-2}$ estimated for the lobes of typical Seyfert 2s from the nonthermal emission. Hence, we are again forced to the conclusion that either the lobes are either well out of equipartition or else that the lobe plasma contains a significant thermal component.

3. Implications for the ISM of Seyfert Galaxies

Typically Seyfert radio sources are of the order of approximately a kpc in size. This statistic, combined with our inference of the energy flux in the jets required to power the narrow line region, has implications for the density of the confining ISM which we now calculate. These calculations are mainly concerned with the prototype Seyfert 2, NGC 1068, but they are easily applied to any other Seyfert. In this analysis we use the solution for the size of a radio lobe as given by Bicknell, Dopita, & O’Dea (1997) (see also Begelman (1996)). Take x_h to be the size of the lobe (from core to head), x_0 an arbitrary scale length, ambient density $\rho = \rho_0(x/x_0)^{-\delta}$, F_E the jet energy flux, ζ the ratio of lobe pressure near the head to average lobe pressure and t the time, then

$$x_h = x_0 \xi^{1/(5-\delta)} \quad (3-1)$$

where

$$\xi = \frac{(5-\delta)^3 \zeta^2}{18\pi(8-\delta)} \left(\frac{F_E t^3}{\rho_0 x_0^5} \right) = 0.26 \frac{(5-\delta)^3}{(8-\delta)} \frac{F_{E,43} t_6^3}{n_0 (x_0/\text{kpc})^5} \quad (3-2)$$

where $10^{43} F_{E,43} \text{ ergs s}^{-1}$ is the jet energy flux, t_6 Myr is the age, $n_0 \text{ cm}^{-3}$ is the ambient hydrogen density at a radius of x_0 , and, following Begelman (1996) we have taken $\zeta = 2$. For a given size and age the implied density is

$$n_0 = \frac{(5-\delta)^3 \zeta^2}{18\pi(8-\delta)} \left(\frac{F_E t^3}{\rho_0 x_0^5} \right) = 0.26 \frac{(5-\delta)^3}{(8-\delta)} \frac{F_{E,43} t_6^3}{n_0 (x_0/\text{kpc})^5} \left(\frac{x_h}{x_0} \right)^{-(5-\delta)} \quad (3-3)$$

For NGC 1068, the projected size is 700 pc and assuming that this is close to the actual size, we obtain Hydrogen densities of 3.1, 1.3 and $0.4 \times F_{E,43} t_6^3 \text{ cm}^{-3}$ for $\delta = 0, 1$ and 2 respectively. These densities are typical of those inferred for the disk ISM in the inner regions of spiral galaxies (e.g., Wevers (1984), Bosma (1981)). That is, for any reasonable density profile, energy fluxes in the range of $10^{43} - 10^{44} \text{ ergs s}^{-1}$ and dynamical ages $\sim 10^6$ yrs, we have an implied range of densities $\sim 1 - 10 \text{ cm}^{-3}$. This density is typical of what one would infer for most Seyferts and is in principle observable from the diffuse emission surrounding the lobes. Cecil, Bland, & Tully (1990) have determined densities $\gtrsim 10^{2.5} \text{ cm}^{-3}$ from the [SII] lines emitted by ionized gas in NGC 1068. If these measurements represented an average density of the ISM in NGC 1068, then the implied jet energy flux would be substantial ($\sim 10^{45} \text{ ergs s}^{-1}$). However, the ionized gas is likely to be clumpy and if the gas is shocked as we suggest, then the [SII] density is likely to be about a factor of 50 – 100 higher than the pre-shock density, depending upon the magnetic parameter $Bn^{-1/2}$. This puts the pre-shock density into the range suggested by the above dynamical calculation. Thus, the existing ground-based measurements of the [SII] densities in NGC 1068 are consistent with our model but we cannot claim that they constitute definitive support for it. Nevertheless, this analysis and further calculations given below indicate that HST measurements of densities in this and other Seyfert galaxies are certainly of great interest. Mapping of the Faraday rotation structure may also lead to further insights.

4. Implications of the Energy Budget

There have been numerous observations of radio emission in Seyferts which indicate collimated outflow. However, only a few observations have the required sensitivity and resolution to actually detect jets. In the small number of cases that have been observed with sufficient resolution, e.g.. MKN 3 (Kukula et al. 1993), MKN 6 (Kukula et al. 1996), MKN 78 (Pedlar et al. (1989), Whittle & Wilson (1997)), NGC 1068 (Gallimore et al. 1996; Gallimore, Baum, & O’Dea 1996) and NGC 4151 (Pedlar et al. 1993) the jets appear to be initially well-collimated and supersonic and then to disrupt and to become subsonic. In no cases do there appear lobes with bright hotspots as in classical FR2 radio galaxies. However, nearer to the core, jet knots occur, reminiscent of structures associated with shocks in supersonic jets. In NGC 1068, at least one of the radio knots near the core appears associated with an oblique shock where the jet is deflected by a narrow-line cloud. The northern NGC 1068 lobe may well be associated with the end of a subsonic jet and simulations relating to this situation would be of interest. Thus, dynamically Seyfert jets resemble FR1 jets which appear to be initially supersonic and relativistic and to then undergo a transition to turbulent transonic flow. At this transition FR1 jets are mildly relativistic with $\beta = v/c \approx 0.6 - 0.7$ (Bicknell 1994; Bicknell 1995). The question then arises, are Seyfert jets also mildly relativistic in the region 10 – 100 pc from the core?

Using the data in the above-cited papers it is possible to begin to address this question. In the following we assume that the [OIII] luminosity is the result of interaction of each jet with the ISM, i.e. the luminosity of the [OIII] λ 5007 line associated with one jet (i.e. one side of the NLR) is given by

$$L([\text{OIII}]) \approx 0.02 (1 - f_{\text{ad}}) F_{\text{E}} \quad (4-1)$$

where $f_{\text{ad}} \sim 0.5$ is the adiabatic factor mentioned above, the factor of 0.02 is the approximate fraction of the total emission line and continuum luminosity emitted in the λ 5007 line (cf. Bicknell, Dopita, & O’Dea (1997)) and, as above, F_{E} is the jet energy flux. We use the energy flux inferred from this equation together with the [OIII] λ 5007 luminosities on the jet side to estimate the jet β using

$$F_{\text{E}} = 4p\Gamma^2\beta c A_{\text{jet}} \left[1 + \frac{\Gamma - 1}{\Gamma}\chi \right] \quad (4-2)$$

$$= 3.6 \times 10^{42} \left[\frac{p}{10^{-8} \text{ dyn cm}^{-2}} \right] \left[\frac{r_{\text{jet}}}{10 \text{ pc}} \right]^2 \Gamma^2\beta \left[1 + \frac{\Gamma - 1}{\Gamma}\chi \right] \quad (4-3)$$

where p is the jet pressure, $\beta = \text{jet velocity}/c$, Γ is the jet Lorentz factor, A_{jet} is the jet cross-sectional area, and $\chi = \rho_{\text{cold}}c^2/4p$ the ratio of cold matter energy density to relativistically dominated enthalpy (Bicknell 1994). In order to obtain indicative estimates of jet velocity, we put p equal to the minimum pressure inferred from the radio images, taking the lower and upper cutoff Lorentz factors to be 10 and 10^4 respectively⁵ We also take $\chi = 1$, since for an initially relativistic

⁵The minimum pressure is relatively insensitive to these assumptions. The use of the minimum pressure here is

jet making the transition to subsonic flow, $\chi \sim 1$ (Bicknell & Begelman 1996). However, the estimated jet velocity is fairly insensitive to values of χ near one.

The indicative estimates of jet velocity and Lorentz factor implied by this procedure as well as the values of parameters used in the calculation are given in Table 1. The column labeled $f([\text{OIII}])$ in the table, is the fraction of the *total* [OIII] luminosity attributed to the jet. In all but galaxy the inferred jet velocities are of order $0.6 - 0.8 c$. These calculations based on the energy budget alone, therefore could be taken to suggest that jet velocities in Seyferts are relativistic on the 10s of parsecs scale and that they are subsequently strongly affected by entrainment. Nevertheless, we discuss significant difficulties with such a proposition in the following section. These are principally based upon analysis of NGC 1068 radio and emission line data which suggest a much larger than minimum pressure in the jet and a larger momentum flux than could be provided by a relativistic jet. If this is the case for all of the jets that we have considered, then the real velocities are much lower.

The exceptional case (Markarian 78) in Table 1 is of interest. Because of the distance of this galaxy, it is only possible to estimate the minimum pressure at ~ 270 pc from the core and our corresponding estimate of the velocity is $0.05 c$, indicating, on the basis of the above assumptions, that the jet has decelerated to a subsonic velocity by this stage. The jet appears to be deflected by an [OIII]-emitting cloud at this distance from the nucleus (Whittle & Wilson 1997) but there is no indication of a radio knot, indicating that the flow is subsonic, consistent with a smaller velocity. This deduction of deceleration is still valid if the pressure is dominated to the same extent by thermal plasma.

As intimated above, energy considerations provide only a partial indication of jet velocities. Therefore, in the next section we consider the constraints placed on jet velocities by observations of jet-cloud interactions. This effectively brings the jet *momentum* budget into consideration.

reasonable since, if the plasma is near equipartition, the total contribution of enthalpy and Poynting flux to the jet energy flux is similar to the contribution implied by equation 4-3 with $p = p_{\min}$.

5. The Momentum Budget from Jet-Cloud Interactions

5.1. General considerations

In a jet-cloud interaction as schematically indicated in Figure 3, a supersonic jet is deflected by a cloud producing an oblique shock in the jet. The post-shock pressure drives a shock into the cloud which, if the cloud is dense enough, is fully radiative. The situation depicted in Figure f:jet-cloud is an oversimplification since the surface of the cloud will not remain flat but will be "gouged out" by the jet and also become filamentary – both as a result of the action of the Kelvin-Helmholtz instability. This will especially be the case if the post-shock flow is subsonic. In essence the force applied by the jet to the cloud is a fraction of the jet momentum flux and the estimates of shock luminosity presented below based on this idealized model probably underestimate this fraction. Nevertheless, the various parametric estimates we make below are probably indicative and motivate further numerical work on this topic.

Given our idealized model, let us take p_{sh} to be the post-oblique shock pressure in the jet and ρ_{cl} to be the density of the cloud. The radiative shock driven into the cloud has a velocity, $V_{\text{sh}} \approx (4p_{\text{sh}}/3\rho_{\text{cl}})^{1/2}$ which together with the density and shock area determines the line fluxes from the cloud. Since $p_{\text{sh}} \propto \rho_{\text{jet}} V_{\text{jet}}^2$ then the force exerted by the shock on the cloud, $p_{\text{sh}} A_{\text{sh}}$ (where $A_{\text{sh}} \text{ cm}^2$ is the shock area) is proportional to the jet *momentum* flux. We estimate the various coefficients of proportionality as follows.

We parameterize the oblique shock by the pre-shock Mach number, M_{jet} , of the incident jet and the deflection angle, $\Delta\theta$, of the jet, the latter being constrained by observations. We take θ_1 and $\theta_2 = \theta_1 + \Delta\theta$ to be the usual angles between the pre- and post-shock flow and the shock normal and $M_x = M_{\text{jet}} \cos \theta_1$ to be the normal component of Mach number. Using the Rankine-Hugoniot conditions for a non-relativistic jet, one can readily show that

$$\tan \Delta\theta = \frac{2(M_x^2 - 1) \tan \theta_1}{M_x^2 [(\gamma - 1) + (\gamma + 1) \tan^2 \theta_1] + 2} \quad (5-1)$$

where $\gamma = 5/3$ is the ratio of specific heats. Given M_{jet} and $\Delta\theta$ this equation can easily be solved numerically for θ_1 and then all of the other shock parameters, in particular,

$$\frac{p_{\text{sh}}}{\rho_{\text{jet}} V_{\text{jet}}^2} = \frac{1}{\gamma M_{\text{jet}}^2} + \frac{2}{\gamma + 1} \left[\cos^2 \theta_1 - \frac{1}{M_{\text{jet}}^2} \right] \quad (5-2)$$

The luminosity from shock excited emission lines is proportional to the shock area and we therefore need to relate the shock area to the area of the jet. As we show in Figure 3 this is determined by the addition of x_1 , the projection of the shock onto the cloud and x_2 , the distance traveled by the jet before a sound wave emitted from the edge of the jet intercepts the cloud. The total distance is given by

$$x_1 + x_2 = D_{\text{jet}} \sec \theta_1 (\sin \theta_2 + M_2 \cos \theta_2), \quad (5-3)$$

where M_2 is the post-shock Mach number, readily calculated from the Rankine-Hugoniot equations. The ratio of cloud shock area to jet cross-sectional area is given by $A_{\text{sh}}/A_{\text{jet}} \approx (x_1 + x_2)/D_{\text{jet}}$. Expressing the jet momentum flux, approximately in terms of the energy flux by

$$\rho_{\text{jet}} V_{\text{jet}}^2 A_{\text{jet}} = \frac{2F_{\text{E}}}{V_{\text{jet}}} \left[1 + \frac{2}{(\gamma - 1)M_{\text{jet}}^2} \right]^{-1}, \quad (5-4)$$

we have for the force exerted by the shock:

$$p_{\text{sh}} A_{\text{sh}} \approx \frac{2F_{\text{E}}}{V_{\text{jet}}} f(M_{\text{jet}}, \Delta\theta) \quad (5-5)$$

where

$$f(M_{\text{jet}}, \Delta\theta) = \frac{p_{\text{sh}}}{\rho_{\text{jet}} V_{\text{jet}}^2} \left[1 + \frac{2}{\gamma - 1} \frac{1}{M_{\text{jet}}^2} \right]^{-1} \sec \theta_1 [\sin \theta_2 + M_2 \cos \theta_2] \quad (5-6)$$

and the jet velocity is given by:

$$\beta_{\text{jet}} = \frac{V_{\text{jet}}}{c} \approx \frac{2F_{\text{E}}}{p_{\text{sh}} A_{\text{sh}} c} f(M_{\text{jet}}, \Delta\theta). \quad (5-7)$$

The factor $f(M_{\text{jet}}, \Delta\theta)$ is easily estimated from the Rankine-Hugoniot conditions and a plot of this parameter as a function of Mach number for different deflections (suggested by the projected deflection at NLR-C) is given in Figure 4. Interestingly, the variation of $f(M_{\text{jet}}, \Delta\theta)$ with Mach number is minor and there is not a great variation with deflection angle. The physical parameter $2F_{\text{E}}/(p_{\text{sh}} A_{\text{sh}} c)$ can be determined from the energy flux required to power the optical emission excited by the lobe expansion and the parameters of the radiative shock in the dense cloud as shown below in the specific case of NGC 1068.

In Figure 4 we also show the ratio of post-shock to pre-shock pressure as a function of Mach number. This is used in the following discussion of NGC 1068.

5.2. Application to NGC 1068

Using Merlin and VLA images together with an HST FOC [OIII] λ 5007 image of NGC 1068, Gallimore, Baum, & O’Dea (1996) have shown that a significant number of emission line clouds lie adjacent to the Northern jet in NGC 1068, in particular clouds NLR-C, NLR-D and NLR-F. The cloud NLR-G lies along the projected direction of the jet which may be too faint at this position to show a knot. The projected areas of these clouds are all of order 10^{40} cm². These emission line clouds constitute an excellent example of where jet-cloud interactions are responsible for the excitation of at least part of the narrow line region and the following analysis aims to determine parameters for the radiative shocks which we assume exist in these clouds. In particular we are interested in the parameters of the cloud NLR-C near which the radio jet has a prominent radio knot (knot C). The jet also suffers a clear deflection $\approx 23^\circ$ at this location. Our interpretation of

the associated jet and narrow-line cloud morphology is that the deflection of the jet by NLR-C leads to the situation analyzed above, namely the production of an oblique jet shock and the driving of a radiative shock into the cloud by the associated pressure.

For shocks in the velocity range of $500 - 1000 \text{ km s}^{-1}$ the $H\alpha$ luminosity is given in terms of the Hydrogen density $n_H \text{ cm}^{-3}$, the shock area $A_{\text{sh}} \text{ cm}^2$ and the shock velocity, V_3 thousand km s^{-1} , by

$$L(H\alpha) = 5.3 \times 10^{-3} n_H A_{\text{sh}} V_3^{2.41} \text{ ergs s}^{-1} \quad (5-8)$$

The pressure driving the shock, p_{sh} is given in terms of the cloud density, ρ_{cl} and the shock velocity, V_{sh} , by $p_{\text{sh}} \approx \rho_{\text{cl}} V_{\text{sh}}^2$ so that the shock force is

$$p_{\text{sh}} A_{\text{sh}} \approx \rho_{\text{sh}} V_{\text{sh}}^2 \approx 4.5 \times 10^{-6} V_3^{-0.41} L(H\alpha) \quad (5-9)$$

Here we use the observed velocity dispersion $\sim 1000 \text{ km s}^{-1}$ in the NLR of NGC 1068 as an estimate of the shock velocity.

The $H\alpha$ flux used in the above expression was estimated as follows: The HST $H\alpha$ filter transmits (redshifted) [NII] λ 6548 and [NII] λ 6583 and we took the transmission curve of this filter into account to obtain an estimated $H\alpha$ flux of $F(H\alpha + [NII]) / (1 + 0.74R)$ where R is the ratio of [NII] λ 6583 to $H\alpha$. The shock models in the velocity range $500 - 1000 \text{ km s}^{-1}$ imply that $R \approx 0.75$ so that we have used this value. Table 1 contains the measured $H\alpha + [NII]$ and [OIII] fluxes in the brightest regions of the narrow line clouds as well as the [OIII]: $H\alpha$ ratio. In principle one could use the velocity dependence of this ratio to estimate the shock velocity. However, the [OIII] flux is metallicity-dependent. Moreover, the high measured values of [OIII]: $H\alpha$ suggest to us that the observed [OIII] line flux may be dominated by the shock precursor region. In table 3, therefore, we give estimates of number density, shock pressure and shock force for two shock velocities, 500 and 1000 km s^{-1} . The first two quantities are for a nominal shock area of 10^{40} cm^2 . As equation (5-8) implies the number density estimate depends fairly strongly on the assumed shock velocity but is clearly in the vicinity of a few hundred cm^{-3} – typical of molecular cloud densities. The shock pressure is much less sensitive (see equation (5-9) and is in the vicinity of a few $\times 10^{-6} \text{ dynes cm}^{-2}$ for shock areas $\sim 10^{40} \text{ cm}^2$. The shock force, of course, has the same velocity dependence as the pressure and is independent of the shock area. This is the parameter of primary importance here since it is the shock parameter which enters into the jet velocity estimate (see equation (5-7)).

A clear prediction from these estimates is that densities measured from the [SII] lines should be in the vicinity of 10^{3-4} cm^{-3} because of the density of the [SII] emitting region relative to the pre-shock density referred to earlier.

Given the parameters in tables 1 and 2, the velocity of the jet near NLR-C is estimated to be

$$\beta_{\text{jet}} \approx \frac{2 \times 10^{44}}{6 \times 10^{34} c} \times f(M_{\text{jet}}, \Delta\theta) \approx 0.1 \times f(M_{\text{jet}}, \Delta\theta)$$

For a plausible range of deflections $\approx 10^\circ - 30^\circ$ relevant to this particular jet-cloud interaction, $f(M_{\text{jet}}, \Delta\theta) \sim 0.4 - 0.8$ (see Figure 4) so that the jet velocity $\sim 0.04 - 0.08 c$. This velocity could

be significantly *increased* if we have underestimated the jet energy flux required to power the NLR or if we have overestimated the force of the radiative shock responsible for the luminosity of NLR-C or if we have underestimated the fraction of jet momentum flux that drives the radiative shock. If, for example, the value of the parameter $f(M_{\text{jet}}, \Delta\theta)$ used above were a factor of two higher than we have estimated here, then the jet velocity would be a factor of two higher. Thus a jet velocity, $v_1 \approx 0.2 - 0.3 c$, before knot C would not be out of the question. In view of this factor of two uncertainty in the estimation of physical parameters further numerical simulations of this process would be useful as would more detailed spectral observations of the NLR of NGC 1068. The latter would assist us to better estimate the parameters of the radiative shocks involved. Despite these reservations, this calculation demonstrates how the combination of total narrow-line region luminosities and individual cloud luminosities associated with jet-cloud interactions can be used to derive jet velocities. It will be interesting to see similar calculations applied to a sample of Seyferts in which the individual uncertainties in various parameters would statistically average out. We also add that it would be unlikely that we have estimated quantities so poorly that the above velocity is in error by an order of magnitude and that the jet velocity is in fact close to c and that the Lorentz factor is large.

Another important feature arising from this analysis is that the shock driving pressure is larger, by about a factor of 40, than the minimum pressure inferred from the radio image and this factor is so large that even given the uncertainties of the above analysis, it is significant. This cannot be an effect of resolution since the shocked region of the jet adjacent to the cloud should be extended by 2-3 jet diameters in the jet direction (the observed elongation based upon the 20 cm. image is about 2 jet diameters) so that the entire post-shock region should be resolved. Moreover, departures from minimum conditions of this amount are unlikely. Rather, this is another indication that there is an additional component of the jet pressure. We can now consider the implications of this by returning to the energy flux. Constraints derived from this can be used to estimate the jet Mach number, as follows. For a nonrelativistic jet the energy flux can be expressed in the form:

$$F_E \approx \frac{\gamma}{\gamma - 1} p V_{\text{jet}} A_{\text{jet}} \left[1 + \frac{\gamma - 1}{2} M_{\text{jet}}^2 \right], \quad (5-10)$$

where γ is the ratio of specific heats. For a pressure, $p = 10^{-6} p_{-6} \text{ dyn cm}^{-2}$ $V_{\text{jet}} \approx 0.06 c$, $D_{\text{jet}} \approx 18 \text{ pc}$ and $\gamma = 5/3$,

$$F_E \approx 1 \times 10^{43} p_{-6} \left(1 + \frac{M_{\text{jet}}^2}{3} \right). \quad (5-11)$$

The pressure here is the *pre-shock* pressure, for which we have no direct estimate. However, given that the *post-shock* pressure $\approx 6 \times 10^{-6} (A_{\text{sh}}/10^{40} \text{ cm}^2)^{-1}$ and that the jet energy flux, $F_E \approx 10^{44} \text{ ergs s}^{-1}$ the ratio of post-shock to pre-shock pressures, p_2/p_1 is given by

$$\frac{p_2}{p_1} \approx C \left(1 + \frac{M_{\text{jet}}^2}{3} \right) \left(\frac{A_{\text{sh}}}{10^{40} \text{ cm}^2} \right)^{-1}, \quad (5-12)$$

where $C \approx 0.6$. The area of the radio knot adjacent to NLR-C ($\approx 5 \times 10^{39} \text{ cm}^2$) indicates that the

actual area of the shock may be less than the nominal shock area (10^{40} cm²). Therefore, in the right panel of Figure 4 we have superposed plots of equation (5-12), for $C = 0.6$ and 1.2 , on the plots of the theoretical shock pressure ratios. Allowing C to vary by a factor of 2 also allows for errors in the estimates other quantities such as the velocity and energy flux which are not known to better than a factor of 2.

It is evident from the intersection of equation (5-12) with the calculated shock pressure ratios that a low, but supersonic jet Mach number ~ 1 – a few is favored. This is consistent with the morphology of this jet: The occurrence of knots, which it is natural to associate with shocks, is indicative of supersonic flow; however the jet spreads at the rate that we associate with turbulent transonic flow. Moreover, it is not as well-collimated as we would expect of a highly supersonic jet.

Given the Mach number and velocity, the sound speed and hence the temperature of the jet can be estimated, with the result that $T = (\mu m_p c^2 / (\gamma k)) M_{\text{jet}}^{-2} \beta_{\text{jet}}^2 = 4.1 \times 10^{12} M_{\text{jet}}^{-2} \beta_{\text{jet}}^2$ K. For $\beta_{\text{jet}} \approx 0.06$, $T \approx 1.5 \times 10^{10} M_{\text{jet}}^{-2}$ K and if $M_{\text{jet}} = 3$, for example, $T = 1.6 \times 10^9$ K. Thus the electrons are mildly relativistic and the protons are subrelativistic, assuming that they are at the same temperature. Thus, although the particle energies are not ultrarelativistic, they are extreme, and must be related to the plasma environment near the black hole.

The mass flux, \dot{M} , in the jet is also of interest. This is given by

$$\dot{M} = \frac{2F_E}{V^2} \left[1 + \frac{2}{(\gamma - 1)M_{\text{jet}}^2} \right]^{-1} = 1 M_{\odot} \text{ yr}^{-1} \left(\frac{F_E}{10^{44} \text{ ergs s}^{-1}} \right) \left[1 + \frac{3}{M_{\text{jet}}^2} \right]^{-1}. \quad (5-13)$$

For values of the jet Mach number, $M_{\text{jet}} = 1, 2$ and 3 , the implied mass fluxes are $0.3, 0.6$ and $0.7 M_{\odot} \text{ yr}^{-1}$, respectively. These estimates are all about an order of magnitude larger than the mass accretion rate rate, $\sim 0.05 M_{\odot} \text{ yr}^{-1}$, onto the black hole estimated from the bolometric luminosity $\sim 3 \times 10^{44} \text{ ergs s}^{-1}$ (Gallimore et al. (1996) corrected for our assumed distance of 15 Mpc) and assuming an efficiency factor of 0.1. This accretion rate is close to the estimate $0.04 M_{\odot} \text{ yr}^{-1}$ of Maloney (private communication) derived from the properties of the maser emission. The discrepancy between the jet mass flux and the accretion rate is a clear indication that most of the jet mass flux is the result of entrainment and given the substantial amount of dense matter in the circumnuclear environment of NGC 1068, this is not surprising. This raises the question as to whether the *initial* velocity of the jet could be relativistic. To answer this we consider the implications of momentum and energy conservation in a relativistic entraining flow. In view of our above deductions concerning the composition of the jet plasma, we assume that the jet is thermally dominated and that initially, the energy and momentum fluxes are dominated by the rest-mass inertia. Hence the initial energy and momentum fluxes ($F_{E,1}$ and $F_{p,1}$ respectively) are given by

$$F_{E,1} \approx (\Gamma_1 - 1) \dot{M}_1 c^2 \quad (5-14)$$

$$F_{p,1} \approx \Gamma_1 \dot{M}_1 c \beta_1 \quad (5-15)$$

where β_1 is the initial value of v/c , Γ_1 is the initial bulk Lorentz factor and \dot{M}_1 is the initial flux

of rest mass. The energy flux is conserved, irrespective of entrainment. If the ambient pressure gradient does not have a major effect on the momentum flux (as is the case when the Mach number is high), then it also is approximately conserved. Thus the ratio of these two quantities is also conserved. When the flow becomes subrelativistic the ratio of energy to momentum flux is $V_{\text{jet}}/2(1 + 3/M_{\text{jet}}^2)$ so that

$$\frac{(\Gamma_1 - 1)c}{\Gamma_1 \beta_1} \approx \frac{1}{2} v \left(1 + \frac{3}{M^2} \right) \quad (5-16)$$

and the initial velocity is determined by the velocity and Mach number at knot C by

$$\frac{\Gamma_1 - 1}{\Gamma_1 \beta_1} \approx \beta_{\text{jet}} \frac{1 + 3/M_{\text{jet}}^2}{2} \quad (5-17)$$

The nonrelativistic limit of this equation is

$$\beta_1 \approx \beta_{\text{jet}} \left(1 + \frac{3}{M_{\text{jet}}^2} \right) \quad (5-18)$$

These equations imply that for a transonic Mach number $\sim 1 - 2$ near knot C the initial velocity of the jet is about 2-4 times higher, i.e. about $0.1 - 0.3c$, given our above estimates. As we have outlined above, it is not unreasonable to envisage “factor of order unity” changes in the parameters of the radiative shock, jet energy flux and the fraction of the jet momentum flux driving the radiative shock that have gone into the estimate of the jet velocity at knot C. Moreover, if the background pressure gradient increases the momentum flux, in the transonic regime of the jet, then equation (5-17) underestimates the jet velocity on the tens of parsecs scale, with the result that the initial jet velocity could be higher. (This can be seen more clearly from equation (5-16) with \approx replaced by \gtrsim .) Thus it is reasonable to conclude that the initial jet velocity in NGC 1068 is mildly relativistic and this is what we expect from a flow ejected from, say within 10 gravitational radii of a black hole. However, it is unlikely that the Lorentz factor is of order a few–10, as in radio galaxies and quasars.

The following considerations of the mass flux enable us to relate the jet properties to that of the corona above the nuclear accretion disk. The initial mass flux, $\dot{M} \approx F_E c^{-2} (\Gamma_1 - 1)^{-1}$, i.e. $2F_E E (c\beta_1)^{-2} \approx 4 \times 10^{-3} \beta^{-2} F_{E,44} M_\odot \text{ yr}^{-1}$, in the non-relativistic limit. If the jet is mildly relativistic (say $\beta \sim 0.5$) then the implied mass flux $\sim 0.02 M_\odot \text{ yr}^{-1}$, close to, but less than, the above-estimated mass accretion rate $\sim 0.05 M_\odot \text{ yr}^{-1}$. (The two are equal for $\beta_1 \approx 0.3$.) We suppose that the jet originates from the coronal region of the black hole accretion disc and that the appropriate radius is of order 10 gravitational radii since this is where most of the accretion disc and related coronal dissipation occur. It is now reasonably well-established that the hard X-ray emission from Seyferts is thermally Comptonized emission from an accretion disc corona with an electron temperature, $T_e \sim 50 - 100 \text{ keV}$ and Thomson optical depth, $\tau_T \sim 2$ (Johnson et al. 1997). Adopting a coronal radius $r_c \sim 10$ gravitational radii, then the electron density in the corona,

$$n_c \sim 1.0 \times 10^{11} \tau_T (r_c/10r_g)^{-1} M_7^{-1} \text{ cm}^{-3} \quad (5-19)$$

where $r_g = GM/c^2$ is the gravitational radius for a black hole of mass M , and $10^7 M_7 M_\odot$ is the black hole mass. Assuming that some of the corona is ejected in the form of a mildly relativistic jet of density n_1 , radius $r_1 \sim 10r_g$, and a Lorentz factor Γ_1 then the corresponding mass flux,

$$\begin{aligned} \dot{M}_1 &\approx \pi r_1^2 n_1 \Gamma_1 \beta_1 c \\ &\approx \frac{\pi \mu m_p G^2}{c^3} M^2 \left(\frac{r_1}{10r_g} \right)^2 n_1 \Gamma_1 \beta_1 \\ &\approx 3.5 \times 10^{-2} \tau_T \left(\frac{r_1}{10r_g} \right)^2 \left(\frac{r_c}{10r_g} \right)^{-1} M_7 \left(\frac{n_1}{n_c} \right) \Gamma_1 \beta_1 M_\odot \text{ yr}^{-1} \end{aligned} \quad (5-20)$$

Given that $M_7 \approx 3$ for NGC 1068, assuming that $\tau \approx 2$, that the jet velocity is mildly relativistic (again for argument, say $\beta_1 \sim 0.5$) and also assuming that the jet density $n_1 \sim n_c$ then the initial jet mass flux $\sim 0.1 M_\odot \text{ yr}^{-1}$. This estimate is close to the mass flux estimated from the jet dynamics and any discrepancy could be attributed to the decrease of density from the corona to where the jet terminal velocity is established. Assuming that the jet and coronal radii are similar (i.e. $r_1 \sim r_c$), then our estimate is not very sensitive to our assumptions concerning these parameters. This good order of magnitude agreement motivates closer examination of the relationship between discs, their coronae and the jets ejected from them.

The other issue to address here is the confinement of a jet with a pressure $\gtrsim 10^{-6} \text{ dynes cm}^{-2}$. This is too large a pressure to be provided by a hot interstellar medium; a number density $\gtrsim 700 \text{ cm}^{-3}$ would be required and the cooling from this would be catastrophic. The other possibility, suggested by the observations of Cecil, Bland, & Tully (1990), is that the jet is inertially confined by a dense cool outflowing wind. If the wind has a density $\sim 100 \text{ cm}^{-3}$, the overpressured jet drives shocks into it with a velocity

$$V_{\text{sh}} = 650 \text{ km s}^{-1} \left(\frac{P}{10^{-6} \text{ dynes cm}^{-2}} \right)^{1/2} \left(\frac{n}{100 \text{ cm}^{-3}} \right)^{1/2} \quad (5-21)$$

There is evidence for such shocks from the observations of Axon et al. (1997) who find spectral evidence for line splitting of approximately 1000 km s^{-1} in the gas coincident with the jet (in projection). The presence of the coronal line of [FeVII] $\lambda 3769$ in their spectra is indicative of high excitation. Using the data of Cecil, Bland, & Tully (1990) which indicate a velocity $\sim 1000 \text{ km s}^{-1}$ and an opening cone angle for the wind $\sim 40^\circ$, the mass flux is $\dot{M}_{\text{wind}} \approx 0.8 M_\odot \text{ yr}^{-1}$. (We have evaluated the cross-sectional area at 24 pc, the location of NLR-C.) Again, it is interesting that this mass flux is of order the mass accretion rate. The energy transported by such a wind $\sim 3 \times 10^{41} \text{ ergs s}^{-1}$ and therefore the wind is not competitive with the jet in exciting the narrow-line region.

Finally, we also note here that the jet velocity implied by a conventional (radio galaxy) value of the parameter κ_ν would be unreasonably small. The value of $\kappa_{1.5}$ implied by our calculated jet energy flux $\sim 10^{44} \text{ ergs s}^{-1}$ and the Wilson & Ulvestad (1994) radio flux density, 3.8 Jy, for the linear part of the source is $\kappa_{1.5} \sim 5.5 \times 10^{-15} \text{ Hz}^{-1}$. If $\kappa_{1.5}$ were a factor of $10^3 - 10^4$ higher, say

$\sim 10^{-12} - 10^{-11} \text{ Hz}^{-1}$, the jet energy flux would be a factor of $10^3 - 10^4$ lower and the jet velocity, implied by equation (5-7), would be in the range of $3 - 30 \text{ km s}^{-1}$. Therefore, our interpretation of the jet and associated emission-line morphology, provides additional support for a much lower value of κ_ν in NGC 1068 and consequently for much greater energy input into the NLR than previously supposed. The only way in which this conclusion could be in error would be if the cloud NLR-C were photoionized and its excitation had nothing to do with the deflection of the jet.

6. Discussion

In this paper we have addressed the physics which is necessary in order to support the view that the NLR emission from Seyfert galaxies be powered, at least in part, by the energy and momentum associated with the radio jets. One requires jet energy fluxes $\sim 10^{43-44}$ ergs s^{-1} and a much smaller ratio of radio power to jet energy flux than is normally invoked for radio galaxies. A lower value of this ratio is suggested by the smaller ages of Seyferts compared to radio galaxies. However, we also require that either the magnetic fields in the lobes of Seyferts be sub-equipartition or more likely, that the fraction by energy of relativistic plasma in the lobes be much smaller than in radio galaxies. This raises the question as to where the composition of the jets is established. Are the jets initially relativistic in composition and subsequently diluted by entrainment of thermal plasma from the ISM or are they initially thermally dominated outflows with a small proportion of embedded relativistic gas? If we adopt the first point of view and assume that all AGN jets have initially relativistic velocities and that their internal energies are initially dominated by relativistic plasma, then we infer mildly relativistic velocities in four Seyfert jets mostly within 100 pc of the core. On the other hand, in NGC 1068, additional information provided by a jet-cloud interaction near the core, suggests a lower velocity $\sim 0.04 - 0.08 c$ 24 pc from the core and, in order to maintain the same energy flux, a substantial contribution to the jet pressure from thermal gas is required. As we noted above, the velocity estimate from the parameters of the jet-cloud interaction also support a significantly higher jet energy flux in the northern NGC 1068 jet than previously supposed and therefore support our suggestion of a much lower value of the parameter κ_ν in Seyfert galaxies. A counter to this argument would involve the proposition that NLR-C is, in fact, photoionized, and that the deflection of the jet at this point has nothing to do with its excitation. This could be resolved by detailed HST optical and UV spectra of this cloud which could establish whether it is photoionized or shocked (see, for example, Dopita et al. (1997)).

At present the notion that Seyfert jets may not be initially ultrarelativistic in composition, is only based upon the analysis of data on one galaxy, NGC 1068. However, the alternative, that Seyfert jets are dominated by thermal plasma from the outset, is probably more sustainable as a general proposition. If the internal energy of Seyfert jets were relativistically dominated, then one would have to explain why a $\sim 10^{44}$ ergs s^{-1} jet of relativistic plasma produced so little radio emission on kpc scales. Dilution by substantial entrainment of thermal gas and a related energy loss by the relativistic component as it mixes with the thermal plasma may go part way to explaining the low level of extended radio emission. However, a model of this sort may meet substantial physical difficulties. It is far more straightforward to invoke a substantial thermal component from the outset. Nevertheless, whilst we have shown, on the basis of our interpretation that the NGC 1068 jet is probably not dominated by ultrarelativistic particles, the inferred temperature of the NGC 1068 jet, at 24 pc from the core, $\sim 10^9 - 10^{10}$ K is substantial and must be related to the environment of the black hole where it originated. As we have shown, a high pressure jet must interact substantially with its surroundings via shocks and the high excitation

line emission coincident with the jet, discovered by Axon et al. (1997), is good evidence for this. The mass flux in the wind, $\sim 1 M_{\odot} \text{ yr}^{-1}$ is similar to that in the jet at that distance from the core, and is similar to the mass accretion rate onto the black hole.

Work by Colbert (1997) supports the view that Seyfert radio plasma is, at least on large scales, dominated by thermal gas. He finds that, in Seyferts with large-scale outflows, the overwhelming contribution to the lobe pressure is provided by soft X-ray emitting gas, the radio emitting plasma contributing about 1% consistent with our requirements on the energy flux. Dominance of the lobe pressure by ($T \sim 10^7 \text{ K}$), thermal gas has another physical consequence which enhances the self-consistency of our model: The isobaric cooling time for shocked gas, $t_{\text{cool}} \approx 3.6 p_{-9}^{-1} T_7^{2.45} \text{ Myr}$ (where $10^{-9} p_{-9} \text{ dyn cm}^{-2}$ is the pressure and $10^7 T_7 \text{ K}$ is the temperature) indicates lobe cooling time scales \sim a few Myr. This provides an explanation for why the dynamical ages of Seyferts appear to be \sim a few Myr (corresponding to characteristic expansion velocities $\sim 500 \text{ km s}^{-1}$ and sizes $\sim \text{kpc}$). Once the gas in the lobe cools, the lobe collapses and then builds up again over this timescale. Obviously, the gas in the initial region of the jet needs to cool from $\sim 10^9 \text{ K}$ both adiabatically and through mixing in order to reach $\sim 10^7 \text{ K}$.

The paper by Nelson & Whittle (1995) is also of interest in this context. They have shown that when the *total* powers of Seyfert and radio galaxies are plotted against bulge magnitude, the radio galaxies lie well above the sequence defined by the Seyferts. However, restriction to the *core* powers of radio galaxies sees the radio galaxies continuing the Seyfert sequence. That is, when the radio powers of Seyfert and radio galaxies are compared on similar scales, they form part of the same sequence. This suggests that entrainment on the kpc scale may have some influence on the level of kpc-scale radio emission. However, the Seyferts do have, on average, core powers which are lower than those of the radio galaxies consistent with them being weaker radio sources from the outset.

Since the mass flux estimated for the jet at 24 pc from the core exceeds the accretion rate into the black hole by about an order of magnitude, it is likely that the jet mass flux at this point is the result of entrainment. Our estimate the jet velocity near the black hole is subject to the uncertainties in the estimates of jet velocity and Mach number near knot C. However, it is not hard to justify a mildly relativistic velocity. The jet velocity near the black hole is also related to the initial mass flux. If the initial velocity is mildly relativistic then the mass flux is similar to but less than the accretion rate. Moreover, the mass flux is consistent with a typical Seyfert coronal density $\sim 10^{11} \text{ cm}^{-3}$ being ejected at a mildly relativistic velocity. Thus consideration of the NLR excitation has led us to a fundamental linkage between jet properties and the coronal properties of accretion discs.

The remaining point we wish to make is that, for Seyfert jets dominated by thermal plasma, one generally expects a large amount of internal Faraday rotation. For example at knot C in NGC 1068, we calculate a rotation measure of 20,000 rad m^{-2} for an equipartition field $\sim 10^{-3} \text{ G}$. Unfortunately internal jet depolarization is difficult to disentangle from depolarization by the

NLR.

We are grateful to Prof. Mark Whittle and Prof. Andrew Wilson for many helpful discussions over the course of this research, and for access to their data on Markarian 78 before publication. We are also grateful to Dr. S. Baum for helpful discussions on NGC 1068 in the early stages of this work, to Dr. Greg Madejski for providing us with the extremely useful preprint of Johnson et al. (1997) and to Drs. Zdenka Kuncic and Phil Maloney for useful discussions .

REFERENCES

- Anderson, K. S. 1989, *ApJ*, 162, 743
- Axon, D. J., Macchetto, F. D., Winge, C., Marconi, A., & Capetti, A. 1997, *BAAS*, 190, 3916
- Begelman, M. C. 1996, in *Cygnus A: Study of a Radio Galaxy*, ed. C. L. Carilli & D. A. Harris (Cambridge: University Press), 209
- Bicknell, G. V. 1984, in *Physics of Energy Transport in Extragalactic Radio Sources: Proceedings of NRAO Workshop No. 9*, ed. A. H. Bridle & J. A. Eilek (Greenbank, West Virginia: NRAO), 229
- Bicknell, G. V. 1994, *Ap. J.*, 422, 542
- Bicknell, G. V. 1995, *ApJS*, 101, 29
- Bicknell, G. V. & Begelman, M. C. 1996, *ApJ*, 467, 597
- Bicknell, G. V., Dopita, M. A., & O’Dea, C. P. 1997, *ApJ*, 485, 112
- Binette, L., Dopita, M. A., & Tuohy, I. R. 1985, *ApJ*, 297, 476
- Binette, L., Fosbury, R. A. E., & Parker, D. 1993, *PASP*, 105, 1150
- Bosma, A. 1981, *AJ*, 86, 1825
- Capetti, A., Axon, D. J., & Machetto, F. D. 1997, *ApJ*, in press
- Capetti, A., Axon, D. J., Machetto, F. D., Sparks, W. B., & Boksenberg, A. 1996, *ApJ*, 469, 554
- Cecil, G., Bland, J., & Tully, R. B. 1990, *ApJ*, 355, 70
- Colbert, E. 1997. Ph. D. thesis, University of Maryland
- Dopita, M. A., Koratkar, A., Allen, M. G., Ford, H. C., Tsvatanov, Z., Bicknell, G. V., & Sutherland, R. S. 1997, In preparation
- Dopita, M. A. & Sutherland, R. S. 1996a, *ApJS*, 102, 161
- Dopita, M. A. & Sutherland, R. S. 1996b, *ApJ*, 455, 468
- Eilek, J. A. & Shore, S. S. 1989, *ApJ*, 342, 187
- Falcke, H. & Biermann, P. L. 1995, *A&A.*, 293, 665
- Falcke, H., Malkan, M. A., & Biermann, P. L. 1995, *A&A.*, 298, 375
- Gallimore, J. F., Baum, S. A., & O’Dea, C. P. 1996, *ApJ*, 464, 198

- Gallimore, J. F., Baum, S. A., O’Dea, C. P., & Pedlar, A. 1996, *ApJ*, 458, 136
- Gelderman, R. & Whittle, M. 1996, *ApJ*, in press
- Goodrich, R. W. 1992, *ApJ*, 399, 50
- Johnson, W. N., Zdziarski, A. A., Madejski, G. M., Paciesas, W. S., Steinle, H., & Lin, Y. 1997, preprint
- Koekemoer, A. M. & Bicknell, G. V. 1997, *ApJ*, submitted
- Koski, A. T. 1978, *ApJ*, 223, 56
- Kukula, M. J., Gosh, T., Pedlar, A., Schilizzi, R. T., Miley, G. K., Bruyn, de A. G., & Saikia, D. J. 1993, *MNRAS*, 264, 893
- Kukula, M. J., Holloway, A. J., Pedlar, A., Meaburn, J., Lopez, J. A., Axon, D. J., Schilizzi, R. T., & S. A. Baum 1996, *MNRAS*, 280, 1283
- Morganti, R., Killeen, N. E. B., & Tadhunter, C. N. 1993, *MNRAS*, 263, 1023
- Nelson, C. H. & Whittle, M. 1995, *ApJS*, 99, 67
- Pacholczyk, A. G. 1970, *Radio Astrophysics* (San Francisco: Freeman)
- Pedlar, A., Kukula, M. J., Longley, D. P. T., Muxlow, T. W. B., Axon, D. J., Baum, S., O’Dea, C. P., & Unger, S. W. 1993, *MNRAS*, 263, 471
- Pedlar, A., Meaburn, J., Axon, D. J., Unger, S. W., Whittle, D. M., Meurs, E. J. A., Guerrine, N., & Ward, M. J. 1989, *MNRAS*, 238, 863
- Rawlings, S. R. & Saunders, R. 1991, *Nature*, 349, 138
- Storchi-Bergmann, T., Kinney, A. L., & Challis, P. 1995, *ApJS*, 97, 347
- Sutherland, R. S., Bicknell, G. V., & Dopita, M. A. 1993, *Ap. J.*, 414, 510
- Tadhunter, C. N., Morganti, R., Aligheri, diSerego S., Fosbury, R. A. E., & Danziger, I. J. 1993, *MNRAS*, 263, 999
- Viegas, S. M. & Contini, M. 1997, in *Emission Lines in Active Galaxies: New Methods and Techniques*, ed. B. M. Peterson, F.-Z. Chang, & A. S. Wilson (San Francisco: Astronomical Society of the Pacific), 365
- Wevers, B. M. R. 1984. Ph. D. thesis, University of Groningen
- Whittle, M. 1985, *MNRAS*, 213, 189

Whittle, M., A. Pedlar, Meurs, E. J. A., Unger, S. W., Axon, D. J., & Ward, M. J. 1988, ApJ, 326, 125

Whittle, M. J. & Wilson, A. S. 1997, ApJ in preparation

Wilson, A. S. 1997, in Emission Lines in Active Galaxies: New Methods and Techniques, ed. B. M. Peterson, F. Cheng, & A. S. Wilson (San Francisco: Astronomical Society of the Pacific)

Wilson, A. S. & Tsvetanov, Z. I. 1994, AJ, 107, 1227

Wilson, A. S. & Ulvestad, J. S. 1994, ApJ, 263, 576

Table 1: Jet velocities inferred from [OIII] and radio data

Galaxy & Component	Distance to nucleus (pc)	Diameter (pc)	p_{\min} dyn cm ⁻²	$f([OIII])$	$L([OIII])$ ergs s ⁻¹	β	Radio reference Optical reference
Mkn 3 E	69	41	2.6×10^{-8}	0.5	4.8×10^{41}	0.63	Kukula et al. (1993)
Mkn 3 W	141	36	2.0×10^{-8}	0.5	4.8×10^{41}	0.73	Koski (1978)
Mkn 6 4	127	51	5.8×10^{-8}	0.5	1.7×10^{42}	0.63	Kukula et al. (1996) Koski (1978)
Mkn 78 W	271	180	5.7×10^{-8}	1.0 ¹	8.7×10^{41}	0.05	Whittle & Wilson (1997) Whittle & Wilson (1997)
NGC 1068 C	24	18	1.4×10^{-7}	1.0 ²	1.0×10^{42}	0.77	Gallimore et al. (1996) Storchi-Bergmann et al. (1995)
NGC 4151 C1	114	37	9.5×10^{-9}	0.5	2.2×10^{41}	0.71	Pedlar et al. (1993)
NGC 4151 C2	56	20	1.4×10^{-8}	0.5	2.2×10^{41}	0.73	Anderson (1989)
NGC 4151 C5	114	23	1.4×10^{-8}	0.5	2.2×10^{41}	0.82	

¹ [OIII] luminosity of western region of source.

² The entire [OIII] luminosity of NGC 1068 is assigned to the northern region because of the one-sided ionization cone.

Table 2: Observed $H\alpha$ and $[OIII]\lambda 5007$ luminosities

Cloud	$F(H\alpha + [NII])$ ergs cm ⁻² s ⁻¹	$F(H\alpha)$ ergs cm ⁻² s ⁻¹	$\log L(H\alpha)$ ergs s ⁻¹	$F([OIII])$ ergs cm ⁻² s ⁻¹	$\log L([OIII])$ ergs s ⁻¹	$[OIII]/H\alpha$
NLR-C	8.50×10^{-13}	5.47×10^{-13}	40.14	2.03×10^{-12}	40.71	3.7
NLR-D	4.01×10^{-13}	2.58×10^{-13}	39.81	9.00×10^{-13}	40.35	3.5
NLR-F	4.40×10^{-13}	2.83×10^{-13}	39.85	1.50×10^{-12}	40.57	5.2
NLR-G	2.59×10^{-13}	1.67×10^{-13}	39.62	9.99×10^{-13}	40.40	6.0

Table 3: Estimated number densities and shock pressures

Cloud	V_{sh} km s^{-1}	$n_H(A_{\text{sh}}/10^{40} \text{ cm}^2)$ cm^{-3}	$p_{\text{sh}}A_{\text{sh}}$ dynes	$p_{\text{sh}}(A_{\text{sh}}/10^{40} \text{ cm}^2)$ dynes cm^{-2}
NLR-C	500	1500	8.2×10^{34}	8.2×10^{-6}
NLR-D	500	690	3.8×10^{34}	3.8×10^{-6}
NLR-F	500	750	4.2×10^{34}	4.2×10^{-6}
NLR-G	500	440	2.5×10^{34}	2.5×10^{-6}
NLR-C	1000	280	6.2×10^{34}	6.2×10^{-6}
NLR-D	1000	130	2.9×10^{34}	2.9×10^{-6}
NLR-F	1000	140	3.2×10^{34}	3.2×10^{-6}
NLR-G	1000	80	1.9×10^{34}	1.9×10^{-6}

Figure captions

Figure 1: Predicted $[OIII]$ luminosity as a function of 1.4 GHz radio power for values of $\log \kappa_{1.4} = -10, -11, -12, -13$ and -14 overlaid on data for radio-loud objects and Seyfert galaxies. Data are from Gelderman & Whittle (1996) (GW), Tadhunter et al. (1993) and Morganti, Killeen, & Tadhunter (1993) (collectively referred to as TM) and Whittle (1985). Legend: Filled circles – CSS sources from GW; filled squares – CSS sources from TM; open circles – GW FR2 radio galaxies; open squares – TM FR2 radio galaxies; diagonal crosses – GW QSOs; plus signs: TM compact flat spectrum sources; open triangles: TM FR1 radio galaxies; filled hexagons: Seyfert galaxies from Whittle (1985). Upper limits are indicated in the usual way.

Figure 2: The ratio $\kappa_{1.4}$ of radio power at 1.4 GHz to jet energy flux for different values of the age parameter $\tau = f_e f_{\text{ad}} t$. A spectral index of 0.7 and a lower cutoff, $\gamma_0 = 1.0$ have been assumed. However, the value of κ_ν is not very sensitive to these parameters.

Figure 3: This figure defines the parameters of a jet-cloud interaction. The extent of the high pressure post-jet-shock region is determined by the sound wave which propagates towards the cloud from the edge of the jet. This high pressure region drives a radiative shock into the cloud.

Figure 4: The left panel shows the factor $f(M_{\text{jet}}, \theta_1)$ defined by equation (5-6) which parameterizes the force of the post jet-shock region ($p_{\text{sh}} A_{\text{sh}}$) in units of F_E/V_{jet} for jet deflections (10° , 20° and 30°) as indicated. The right panel shows the pressure ratio (solid lines) p_2/p_1 as a function of pre-shock jet Mach number for the given deflections. Superimposed on these curves are dashed curves ($p_2/p_1 = C(1 + M_{\text{jet}}^2/3)$, $C = 0.6$ and 1.2) representing the pressure ratio implied by the radiative shock analysis and the jet energy budget for NGC 1068. Both panels are for a non-relativistic jet with the ratio of specific heats $\gamma = 5/3$.

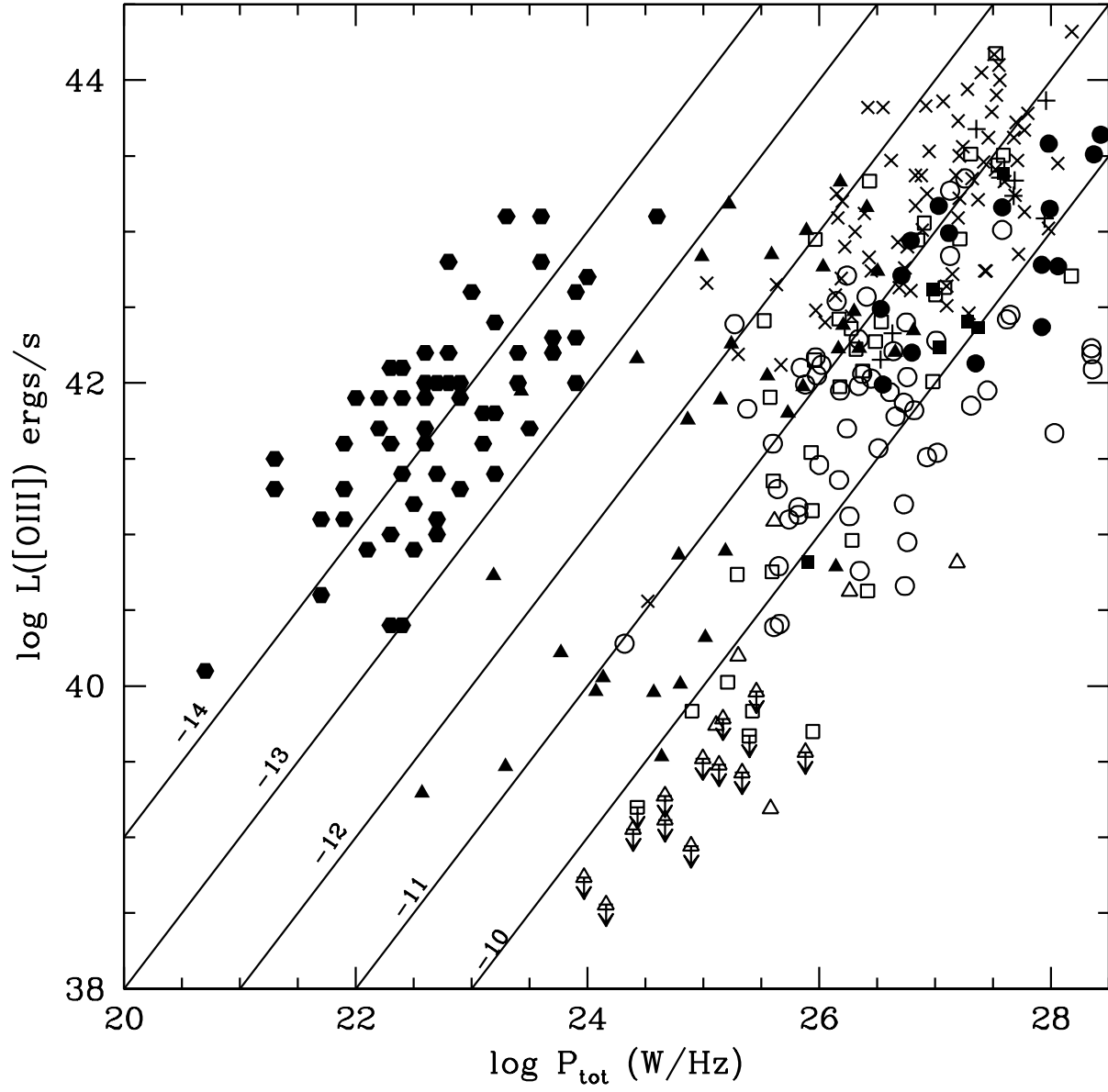


Fig. 1.—

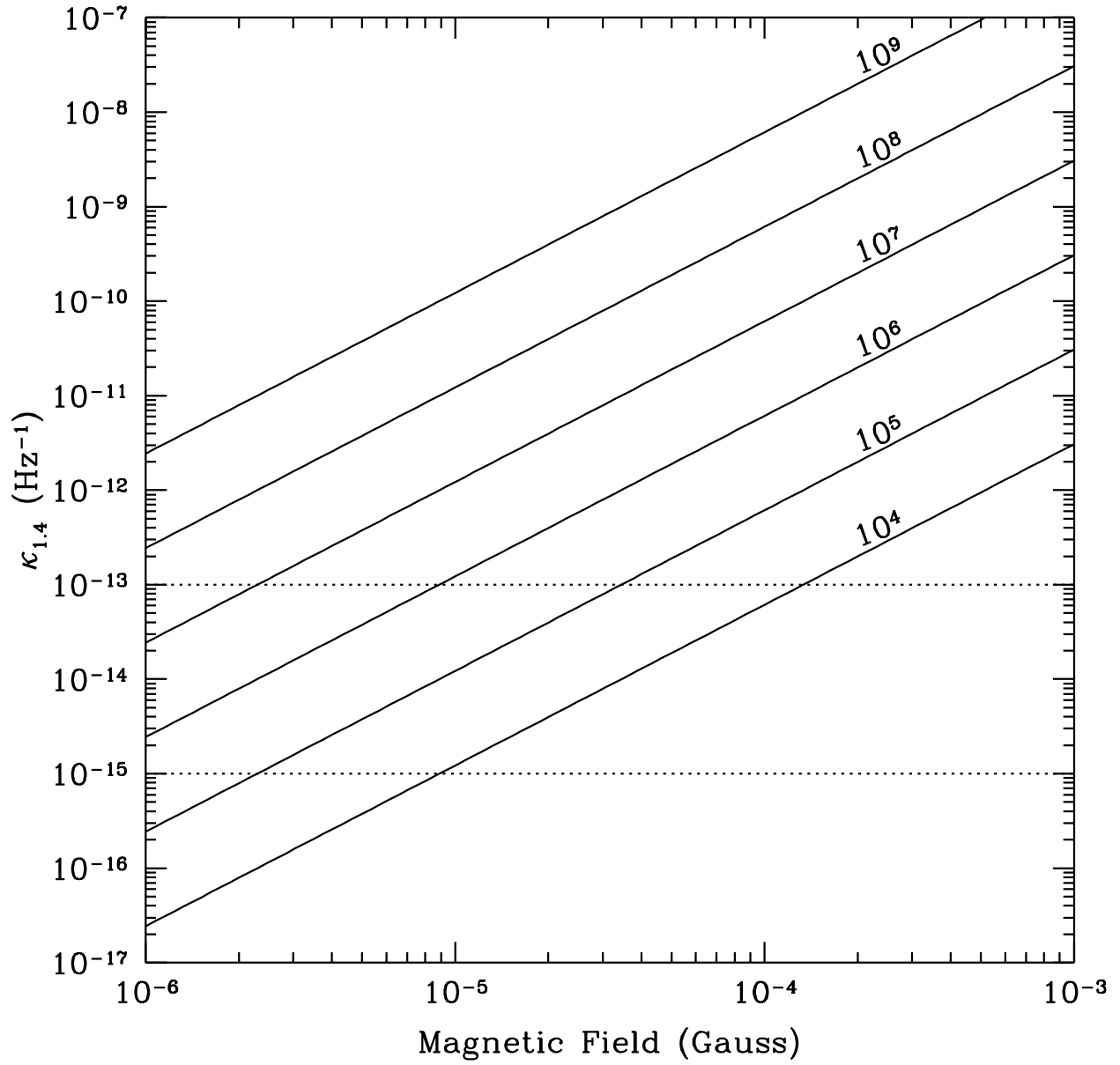


Fig. 2.—

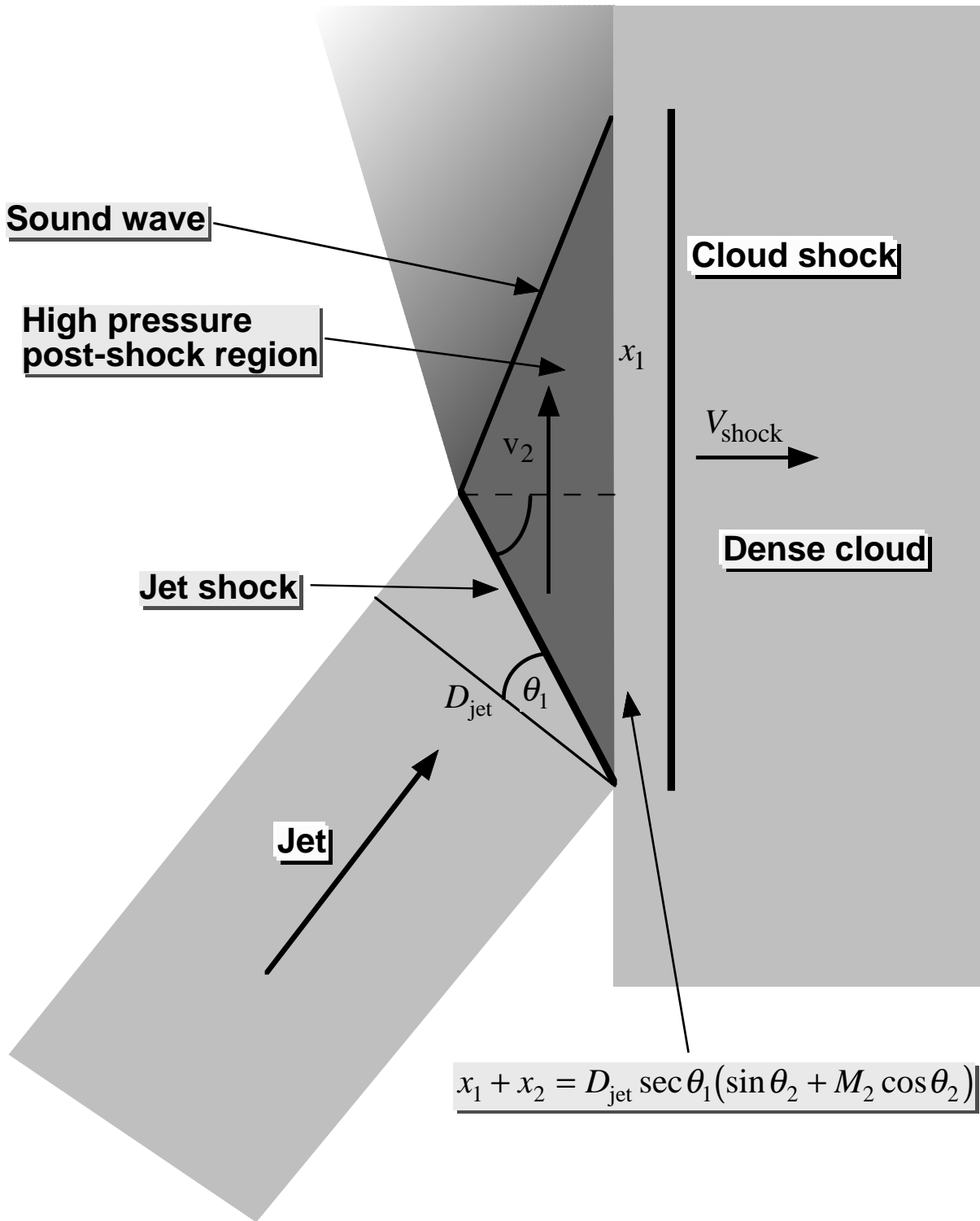


Fig. 3.—

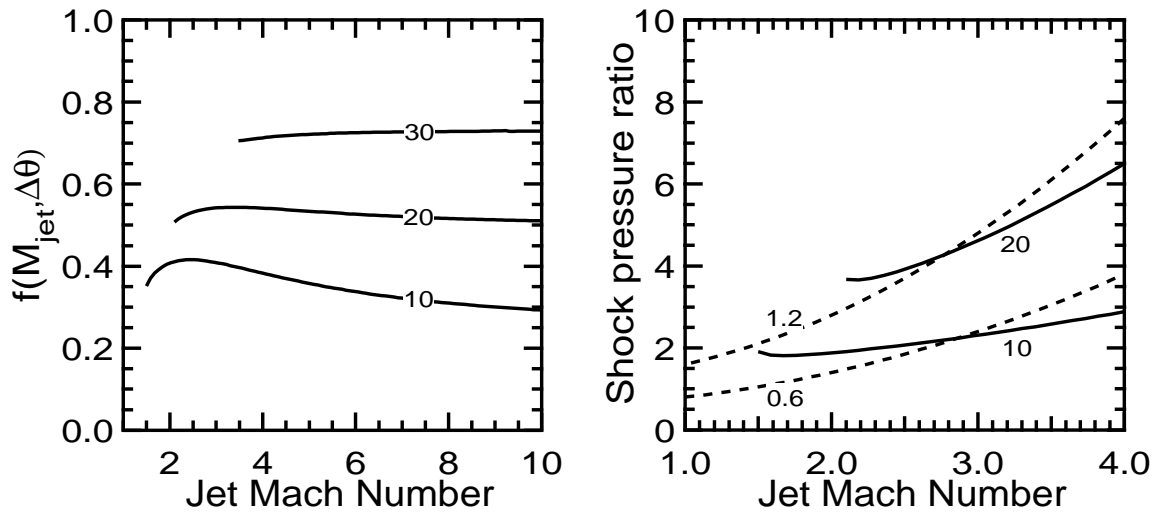


Fig. 4.—